J. Acoust. Soc. Jpn. (*E*) 9, 2 (1988)

Propagation of finite amplitude acoustic waves in layered fluid media
—Normal incidence on the layer—

Tomoo Kamakura,* Manabu Hasegawa,** and Yoshiro Kumamoto*

**University of Electro-Communications,*
1–5–1, Chofugaoka, Chofu, Tokyo, 182 Japan
***Iwatsu Electric Co., Ltd.,*
1–7–41, Kugayama, Suginami-ku, Tokyo, 168 Japan

(*Received 1 July 1987*)

Parabolic approximation is effectively used to analyze the nonlinear acoustic field generated by a directive sound source in layered media. Quasi-linear approach and linear boundary condition are applied to obtain the fundamental and second harmonic waves transmitting through a plane interface that separates two media. The interface is placed in nearfield for the harmonic. The spectral contents of sound pressure are measured and compared with the theoretical prediction. Both the results are in good agreement for propagation curves and beam patterns. Transmission loss by insertion of a thick layer across an acoustic beam is also investigated. It is shown that unlike the fundamental wave loss the harmonic loss varies with source-layer distance. All experiments are conducted in water, methanol and castor oil.

PACS number: 43. 25. Cb, 43. 25. Jh

1. INTRODUCTION

Finite amplitude acoustic wave causes a nonlinear distortion with propagation. This means that many harmonics are progressively generated even if initial wave is purely monochromatic. If the wave travelling in a homogeneous medium reaches an interface where the properties of the medium changes abruptly, various frequency components generated before incidence on the interface might be in part reflected and transmitted.

Previously Wingham *et al.* studied the penetration of a water-sediment interface by a parametric difference frequency beam[1] and Kamakura *et al.* investigated the transmission of parametrically generated audio sound through a sheet of absorptive material in air.[2] In their theories, the transmitted primary and harmonic waves are so much attenuated that new generation of difference frequency wave after transmission is neglected; the parametric array is assumed to be completely truncated at the interface. Rigorously speaking, such assumption does not hold in reality. Particularly, if there should be the interface in nonlinear interaction region or nearfield for secondary wave, the parametric sound generated after transmission might somewhat contribute array formation.

The present paper reports on the transmission of ultrasonic pulse of finite amplitude radiated by a directive sound source through an interface separating two media. The media consist in some liquids and the interface is placed near the source or in the nearfield. In such system, we can not neglect the harmonic generated after the transmission. Since nonlinear boundary conditions negligibly contribute waveform distortion outside a thin boundary layer, linearized boundary conditions can be reasonably applied to derive both the fundamental and second harmonic components.[3] The harmonic generated before incidence on the interface travels through the fluid linearly summing up the newly generated component. We use parabolic approximation for the field analysis because boundary conditions on the source and on the interface are easily imposed.

Theoretical prediction is extensively compared with experiments conducted in water/methanol and water/castor oil systems. The nearfield transmission theory presented here provides numerical results of sound pressure on axis as well as off axis. The problem on transmission loss of finite amplitude sound through a thick layer submerged in water are also considered. Fluid in the layer is methanol or castor oil. Even if the source-layer distance varies, fundamental wave loss is invariant as linear theory predicts. However, the harmonic loss is dependent on the distance. This salient feature is theoretically and experimentally verified.

2. TRANSMISSION THROUGH AN INTERFACE

2.1 Theory

Consider nonlinear acoustic field generated by a circular piston source in a fluid medium. When the source radius a is much larger than wavelength; $ka \gg 1$, where $k=\omega/c_0$, ω is angular frequency and c_0 is the sound speed at small amplitude, the parabolic approximation is used as a convenient tool for nearfield analysis. Let p_1 and p_2 be sound pressures at the fundamental and second harmonic frequencies, respectively. Introducing field quantity q_i, $i=1, 2$, defined by

$$q_i(r, z)=p_i(r, z)\exp[jikz+\alpha_i z] \quad (1)$$

the following parabolic equations for q_i yield[4)]

$$\frac{1}{r}\frac{\partial}{\partial r}\left(r\frac{\partial q_1}{\partial r}\right)-j2k\frac{\partial q_1}{\partial z}=0 \quad (2)$$

$$\frac{1}{r}\frac{\partial}{\partial r}\left(r\frac{\partial q_2}{\partial r}\right)-j4k\frac{\partial q_2}{\partial z}=2\frac{\beta\omega^2}{\rho_0 c_0^4}\exp[-(2\alpha_1-\alpha_2)z]q_1^2 \quad (3)$$

where α_1 and α_2 are the linear sound absorption coefficients of the fundamental and second harmonic waves, ρ_0 is the static density of fluid, r is the radial coordinate and z the axial one. It has been assumed that the field is axisymmetric and quasi-linear approach is applicable to the analysis of nonlinear propagation of finite amplitude acoustic waves. The assumption has also made of the negligible smallness of sound absorption over the wavelength. The solutions of Eqs. (2) and (3) which satisfy the radiation condition in the z direction are given using Hankel transform several times[4)]

$$q_1(r, z)=j\frac{k}{z}\int_0^\infty \exp\left[-j\frac{k}{2}\cdot\frac{r^2+r_1^2}{z}\right] \times J_0\left(\frac{krr_1}{z}\right)q_1(r_1, 0)r_1dr_1 \quad (4)$$

$$q_2(r, z)=-j\frac{\beta k^3}{2\pi\rho_0 c_0^2 z}\int_0^\infty\int_0^\infty\int_0^\pi\int_0^z \frac{\exp[-(2\alpha_1-\alpha_2)z']}{z'} \times\exp\left[-jk\frac{F+4r_1r_2\cos\phi}{4z'}\right] \times\exp\left[-jk\frac{F+4r^2}{4z}\right]J_0\left(\frac{kr\sqrt{F}}{z}\right) \times q_1(r_1, 0)q_1(r_2, 0)r_1r_2dz'd\phi dr_1dr_2 \quad (5)$$

where $F=r_1^2+r_2^2-2r_1r_2\cos\phi$, J_0 is the Bessel function of order zero. Equations (4) and (5) are suitable for arbitrary sound pressure distribution at the source although multiple integral implementation must be done.

Utilization of parabolic approximation above can be easily extended to the field analysis in layered media. Figure 1 shows the geometry of model to be discussed here. We assume that each medium in region (I) and (II) has a homogeneous property and an interface between them is plane to the z axis. According to the empirical results that nonlinear boundary conditions negligibly contribute distortion outside a thin boundary layer, imposition of linearized boundary conditions is safely justified.[8)] Let T_1 and T_2 be linearly obtained transmission coefficients for the fundamental and second harmonic sound pressures, respectively. If multiple wave reflections between the source and the interface do not occur and the transmission coefficients are not dependent on

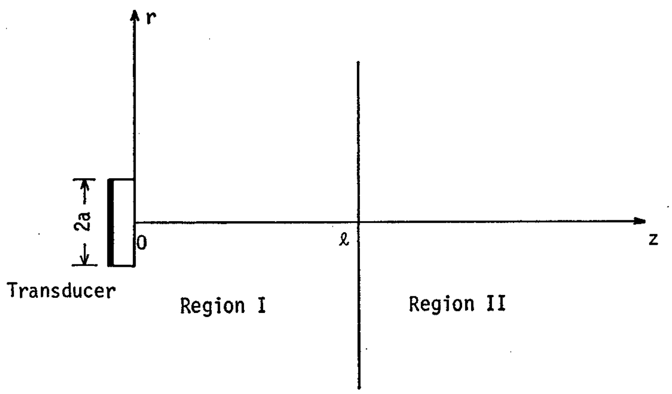

Fig. 1 Geometry of theoretical model.

radial coordinate, wherein the latter assumption holds under the paraxial approximation, then the expression for transmitted fundamental component is

$$\left.\begin{aligned} p_1 &= q_1 \exp[-(jk+\alpha_1)l-(jk'+\alpha_1')(z-l)] \\ q_1 &= j\frac{k'}{z-l}\int_0^\infty \exp\left[-j\frac{k'}{2}\cdot\frac{r^2+s^2}{z-l}\right] \\ &\quad \times J_0\left(\frac{r^2+s^2}{z-l}\right) T_1 q_1(s, l) s ds \\ &= j\frac{k'}{z_t}T_1\int_0^\infty \exp\left[-j\frac{k'}{2}\cdot\frac{r^2+r_1^2}{z_t}\right] \\ &\quad \times J_0\left(\frac{krr_1}{z_t}\right) q_1(r_1, 0) r_1 dr_1 \end{aligned}\right\} \quad (6)$$

where the prime identifies the variables in region (II), l is the distance of the interface from the source and $z_t = z + (k'/k-1)l$.

Next turn to the derivation of second harmonic field in region (II). Since the interface is placed in nonlinear interaction region and wave distortions do not hypothetically occur at the interface, it would be appropriate that the field consists of two wave components; one is the harmonic which has already generated in region (I) and linearly travels through region (II), and the other the newly generated harmonic in region (II). This implies that parametric array produced in each region is additionally connected at the interface and a virtual array is formed. Both the harmonics, p_{21} and p_{22} we denote, are summed up to determine the total harmonic field. By the similar method as the derivation of p_1, p_2 is described in the following forms

$$\left.\begin{aligned} p_2 &= p_{21} + p_{22} \\ p_{21} &= q_{21} \exp[-(j2k+\alpha_2)l-(j2k'+\alpha_2')(z-l)] \\ p_{22} &= q_{22} \exp[-(j2k+2\alpha_1)l-(j2k'+\alpha_2')(z-l)] \\ q_{21} &= -j\frac{\beta k' k^2 T_2}{2\pi\rho_0 c_0^2 z_t}\int_0^\infty\int_0^\infty\int_0^\pi\int_0^l \frac{\exp[-(2\alpha_1-\alpha_2)z']}{z'} \\ &\quad \times \exp\left[-jk\frac{F+4r_1r_2\cos\phi}{4z'}\right] \\ &\quad \times \exp\left[-jk'\frac{F+4r^2}{4z_t}\right] J_0\left(\frac{k'r\sqrt{F}}{z_t}\right) \\ &\quad \times q_1(r_1, 0) q_1(r_2, 0) r_1 r_2 dz' d\phi dr_1 dr_2 \\ q_{22} &= -j\frac{\beta' k'^3 T_1^2}{2\pi\rho_0' c_0'^2 z_t} \\ &\quad \times \int_0^\infty\int_0^\infty\int_0^\pi\int_0^{z-l} \frac{\exp[-(2\alpha_1'-\alpha_2')z']}{z'+k'l/k} \\ &\quad \times \exp\left[-jk'\frac{F+4r_1r_2\cos\phi}{4(z'+k'l/k)}\right] \\ &\quad \times \exp\left[-jk'\frac{F+4r^2}{4z_t}\right] J_0\left(\frac{k'r\sqrt{F}}{z_t}\right) \\ &\quad \times q_1(r_1, 0) q_1(r_2, 0) \\ &\quad \times r_1 r_2 dz' d\phi dr_1 dr_2 \end{aligned}\right\} \quad (7)$$

Increasing the distance l under the condition that the observation point is fixed far from the source, q_{22} becomes small compared with q_{21}. Consequently, p_{21} dominates the harmonic field. When two media are the same, $z_t = z$ and $T_1 = T_2 = 1$, so Eqs. (6) and (7) obviously reduce to Eqs. (4) and (5), respectively.

2.2 Experiments and Discussion

Experiments were carried out in accordance with a block diagram as shown in Fig. 2. The transmitting transducer, whose active radius is 9.5 mm and resonance frequency is 2.4 MHz, radiates tone-burst ultrasounds of finite amplitude with about 6 μs duration. To pick up distorted waves accurately, a wide-band small hydrophone, whose frequency range is available from 2 to 10 MHz, was used. The spectral contents of received signals were obtained by digital Fourier transform. For the sake of precise positioning of the hydrophone, pulse-motors were employed for the movements in r and z directions.

Figures 3 and 4 show the measured and calculated sound pressures of the fundamental and second harmonic components in water alone. Figure 3 gives on-axis SPL at the range from 3 to 20 cm. In order to obtain numerical results, the sound pressure distribution at the source is required. To this end, we measured sound pressure quite near the source and substituted the measured values for the source

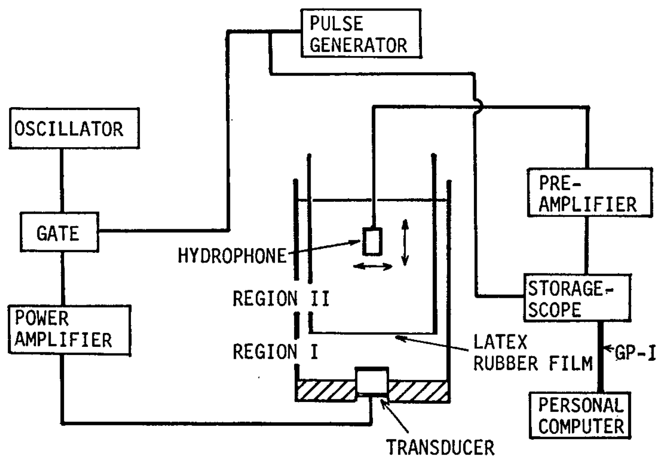

Fig. 2 Block diagram of the experiment.

function of Eqs. (4) and (5). The uniform phase on the source is accounted for. As can be seen in the figure, calculated curves are in good agreement with measured data at the range $z \geq a(ka)^{1/3} \simeq 4.3$ cm, where the parabolic approximation is valid.[4] The second harmonic presents a dip in amplitude at 9.5

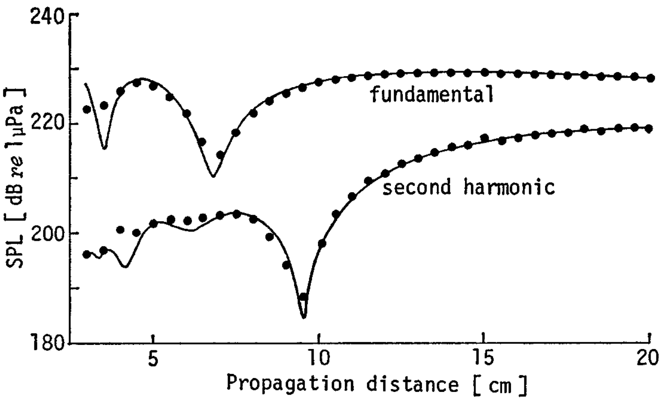

Fig. 3 Fundamental and second harmonic sound pressure levels on the axis of circular piston source in water. Frequency=2.4 MHz, $ka=95.5$, $\alpha_1=0.0015$ neper/cm, $\alpha_2=0.0058$ neper/cm. ●: experiment, ——: theory.

cm, that distance is equal to about 0.21 times the Rayleigh length of the fundamental $ka^2/2 \simeq 45$ cm. The absolute maximum of the pressure seems to be out of range we measured. According to the theoretical prediction, the maximum amplitude is attained at around 25 cm, so our measurement is apparently restricted to nonlinear interaction region or nearfield for the harmonic wave.

The beam patterns at 9, 20 cm are presented in Fig. 4. All pressures are normalized to the fundamental on-axis value. The figure (a) shows complexity of nearfield of the harmonic; pressure on the axis is not necessarily maximum. For comparison, in the figure (b) farfield asymptotic beam pattern (square of the fundamental beam pattern) is also given with a broken line. As can be seen, two theoretical curves almost coincide each other near the axis.

Next, experimental data of finite amplitude sound propagating in two fluid media are presented along with calculated results in Figs. 5~7. We chose two typical layer systems; water/methanol and water/castor oil. For the former system, not only acoustic impedances but also nonlinearity parameters are apparently different for both liquids, whereas for the

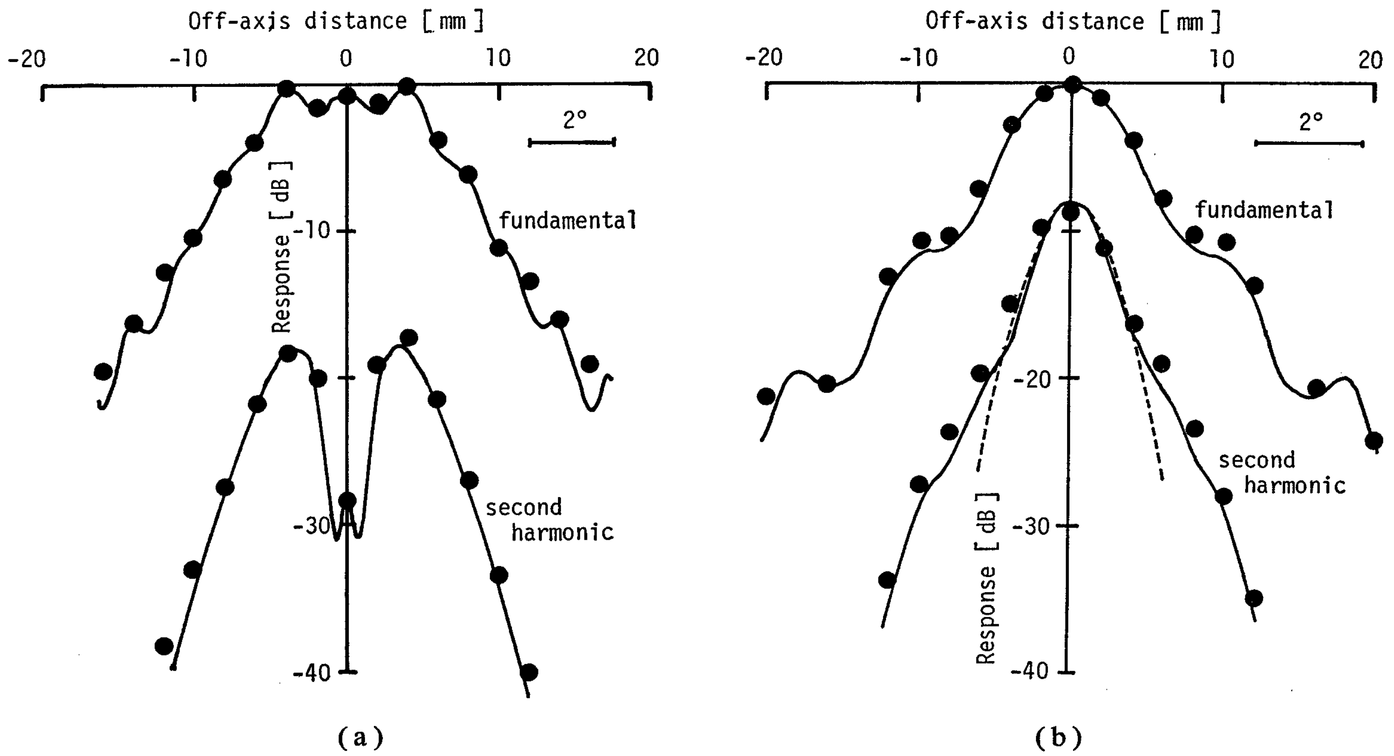

Fig. 4 Fundamental and second harmonic sound pressure beam patterns. ●: experiment, ——: theory. (a) $z=9$ cm, (b) $z=20$ cm. Broken line denotes a farfield asymptotic beam pattern.

Table 1 Physical parameters of water, methanol and castor oil.

Parameter	Liquid		
	Water	Methanol	Castor oil
β	3.48	5.81	5.6
ρ_0 [kg/m³]	998.2	791.3	957.6
C_0 [m/s]	1,483	1,121	1,489
$\rho_0 C_0$ [$\times 10^5$ kg/m²s]	1.48	0.887	1.426

latter system two the impedances are nearly equal. Table 1 represents physical parameters of water, methanol and castor oil.[5,6] In contrast with water and methanol, absorption coefficient of castor oil is large and is severely dependent on temperature. Therefore every measurement we estimated it by means of the most fitted curve to the linear propagation data in castor oil only. Measurements of spectral contents in layered system were excuted by the following procedure. First we measured sound pressures in glass tube of size 8.5 cm in inner diameter and 30 cm in length, filled with water. Thus measured data are circles fully drawn with black in the figures. Next another smaller tube terminated by a latex rubber film at one end to avoid the mixing of liquids was filled with methanol or castor oil, and was inserted into the larger tube (See Fig. 2). Under otherwise unchanged conditions we went on with measurement of sound pressure in region (II). These data are triangles or squares fully drawn with black. In preliminary experiment for water/water system the field disturbance caused by the separating film was ignored.

Figure 5 shows the experimental and calculated results in water/methanol system. The interface existed at 12.2 cm from the source, where the amplitude of ultrasound is still large enough to generate harmonic distortion. As soon as the primary or fundamental frequency wave passes through the interface, its amplitude reduces by 2.5 dB in accordance with impedance mismatch. The harmonic, however, increases during propagation in comparison with the pressure in water alone. This is due to the fact that the nonlinearity parameter and wavenumber in methanol, whose values quantitatively relate to harmonic generation, are larger than those in water. Except that measured pressures of the harmonic near the interface are larger than calculated values

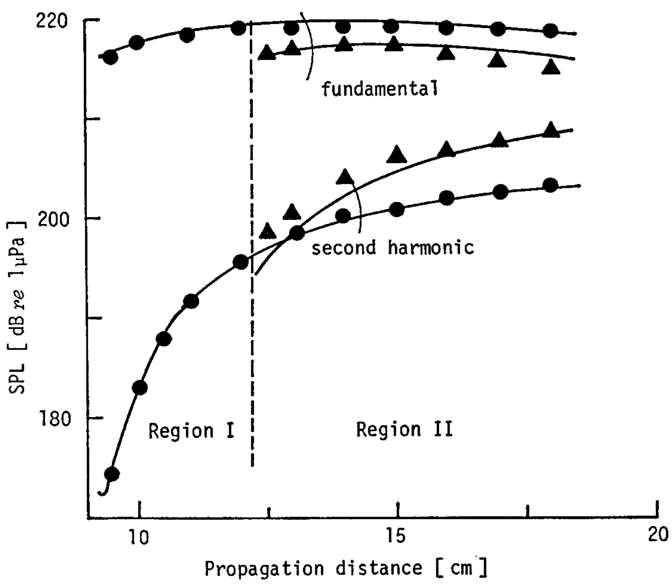

Fig. 5 Fundamental and second harmonic sound pressure levels on the axis in water/methanol system. An interface is placed at 12.2 cm. $\alpha_1'=0.0055$ neper/cm, $\alpha_2'=0.022$ neper/cm. ●, ▲: experiment, ——: theory.

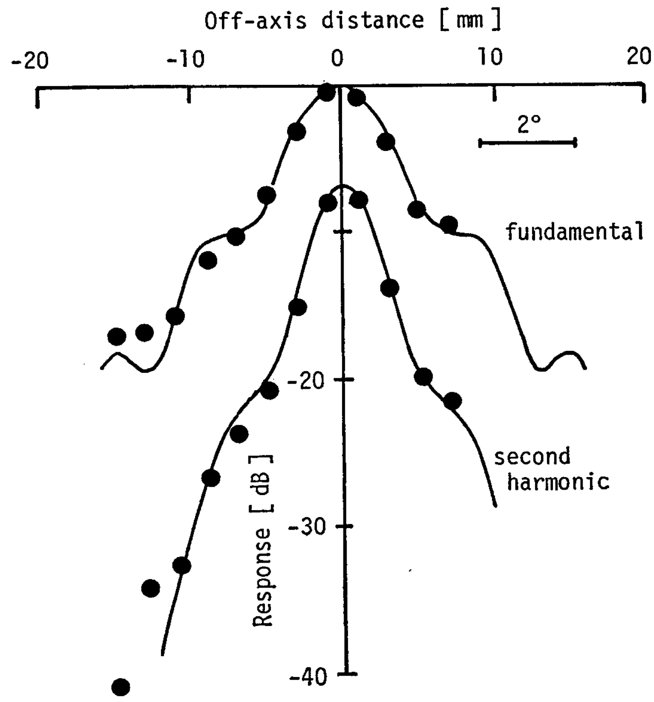

Fig. 6 Fundamental and second harmonic sound pressure beam patterns at 18 cm in water/methanol system. An interface is placed at 12.2 cm. ●: experiment, ——: theory.

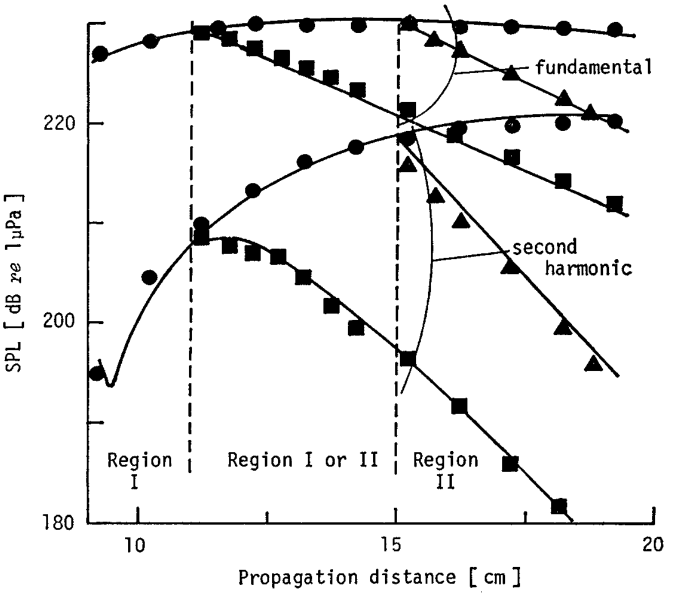

Fig. 7 Fundamental and second harmonic sound pressure levels on the axis in water/castor oil system. An interface is placed at 12 cm or 15 cm. $\alpha_1'=0.26$ neper/cm, $\alpha_2'=0.81$ neper/cm. ●,▲,■: experiment, ——: theory.

by 2～3 dB, agreement between theory and experiment is almost good. Beam patterns at 18 cm from the source are given in Fig. 6. On-axis SPL of the fundamental at that range was around 214 dB *re* 1 μPa. Calculated beam patterns corresponding to the present theory well fit the measured data. In comparison with the results in water alone in Fig. 4, remarkable difference does not appeared.

Sound pressures were measured in water/castor oil as well and are shown in Fig. 7. Data for each range at 12 cm and 15 cm are plotted in the same figure. Compared with water and methanol, sounds attenuate rapidly in castor oil, so the harmonic wave which is continuously transmitted into region (II) does not so much grow up as the case of methanol. However, when the interface approach the source the harmonic intends its amplitude to increase with propagation. This is clearly illustrated in the data for the interface placed at 12 cm.

3. TRANSMISSION THROUGH A THICK LAYER

Imagine that there is multi-layer system between two semi-infinite media and a plane pulse is normally incident on the layers. According to linear theory, total transmission loss is related to sound absorption in each layer and impedance mismatch between layers if exists. This implies that the position (including the width for absorption-free media) for each layer has no effect on the field of transmitted sound. However, as can be estimated by the results of previous chapter, harmonics of finite amplitude sound are generally increased with propagation, so the field is strongly dependent on the layer configuration.

To make clear that point, we consider a simple problem on the transmission of finite amplitude sound beam through a plane layer of finite thickness. It is assumed that the acoustic axis is normal to the layer face and the layer is filled with some fluid different from surrounding water. The theory appropriate for the present problem can be developed by means of parabolic approximation and the authors have already reported the exact equations for the fundamental and second harmonic waves passing

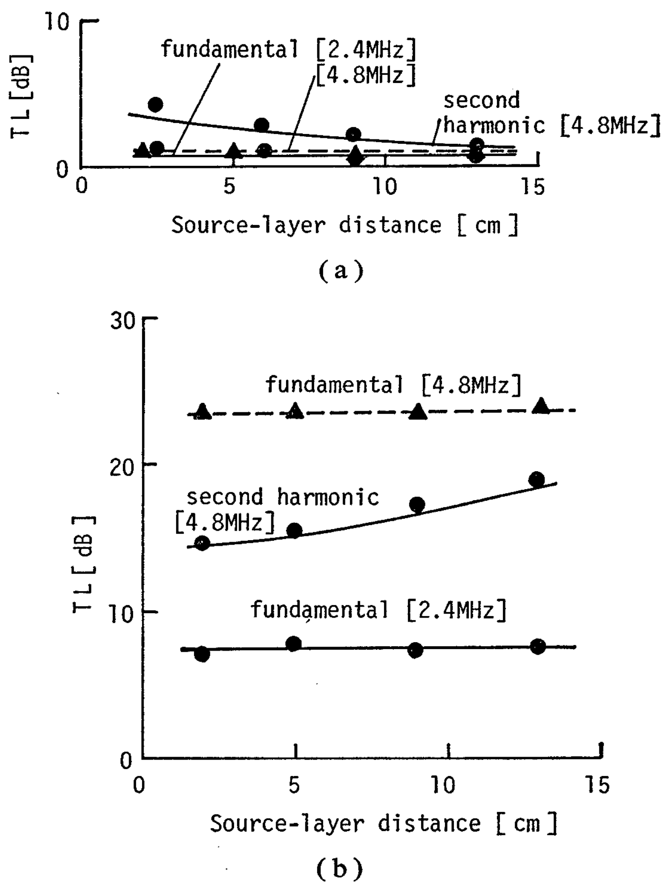

Fig. 8 Transmission losses of fundamental and second harmonic waves. SPLs of the fundamental and second harmonic are 228 dB and 219 dB, respectively. ●,▲: experiment, ——, - - - -: theory. (a) water/methanol/water, (b) water/castor oil/water.

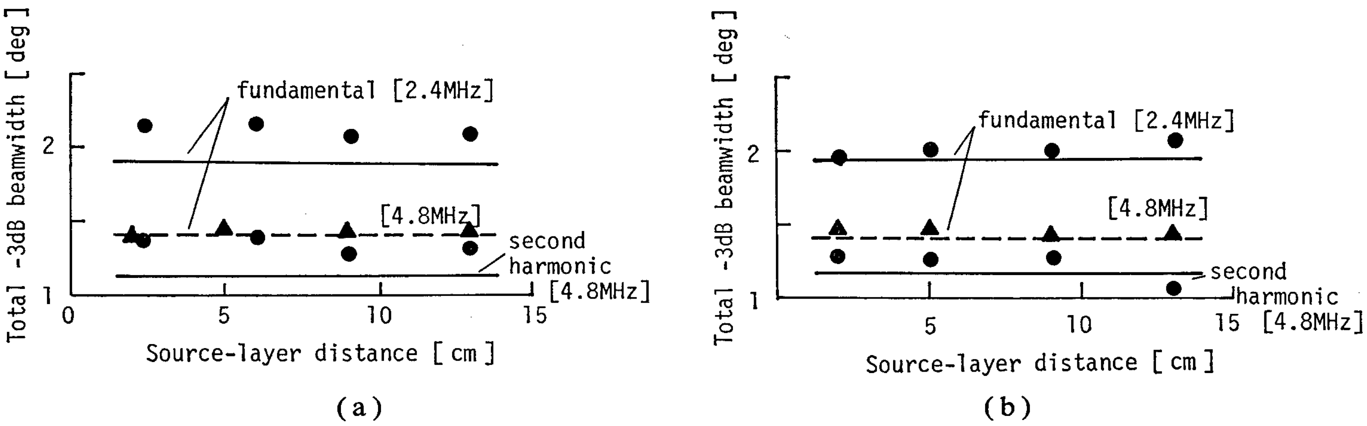

Fig. 9 Total −3 dB beamwidths of fundamental and second harmonic waves. ●,▲: experiment, ——, - - - -: theory. (a) water/methanol/water, (b) water/castor oil/water.

through the layer. The expressions are rather involved and the reader is referred to the work of Shida *et al.* for a full description.[7]

Experimental procedure and conditions are similar to those in Chap. 2 except for using of two rubber films for the separation of liquids. The layer of 2.5 cm in length is filled with methanol or castor oil. Physical parameters of two liquids have been listed in Table 1 and were used for theoretical calculation. Hydrophone was fixed at 18 cm from the source and the distance between the source and front face of the layer was varied at the range from 2 cm to 13 cm. In the absence of the layer, the fundamental and harmonic pressures were 228 dB and 219 dB, respectively. Figure 8 shows the range dependence of transmission loss. For comparison, the loss of using a 4.8 MHz piston source of 6 mm in radius is measured and given in the figures. The frequency is the same as the second harmonic of a 2.4 MHz sound and both the beam patterns are nearly identical. Broken lines are the calculated results for the 6 mm-radius source. As one might see, for fundamental waves of frequency at 2.4 MHz and 4.8 MHz, the transmission loss does not depend on the source-layer distance. The harmonic loss, however, varies with the distance. As the distance is increased, the loss decreases for methanol. The more the layer is apart from the source, the smaller the loss becomes. Whereas, the loss increases for castor oil. Thus different feature of the range-dependence is ascribed to sound absorptions in the layer. For lossy medium like castor oil, the harmonics generated before incidence on the layer and in the layer are much attenuated. Consequently, the harmonic generated after transmission, which reduces its amplitude with the increase of the source-layer distance, results in substantial effect on total transmission loss. In case of small absorption medium such as methanol, to the contrary, the loss is mainly determined by the harmonic component generated before incidence on the layer. It should be noted that within the ranges of our experiment transmission loss for the harmonic in water/castor oil system is less than that for the same frequency wave linearly radiated.

Total −3 dB beamwidths for the fundamental and second harmonic waves are shown in Fig. 9. A noticeable absence in the beam pattern of the second harmonic component is the Westervelt directivity function in parametric array. Even if the array is truncated at any length, the beamwidth hardly changes. This is because that source dimension is much larger than the wavelength the beam pattern is strongly dependent on broad-side array rather than end-fire array of virtual harmonic sources. The reasonable results are appeared in Fig. 9 for both the measured and calculated beamwidths. For methanol, measured data is somewhat large in compared with the calculated values. The reason for the discrepancy is not determined. However, the non-flatness of the film makes probably an effect on the field.

4. CONCLUSIONS

The transmission of finite amplitude acoustic wave by a directive sound source in layered media has been investigated. The present theory developed is based on the parabolic approximation which has been used as a convenient tool for field analysis. Expressions for the fundamental and second harmonic waves transmitting through an interface or a thick layer are somewhat involved, they have well predicted sound pressures on axis as well as off axis at any region where parabolic approximation is valid.

For harmonic wave, truncation of parametric array at some length or virtual connection with some array does not influence on the beam pattern. However, the magnitude of the harmonic is strongly dependent on the array formation and array structure. Phase variation of spectral components, which has not been referred in this paper, is the subject of further investigation.

REFERENCES

1) D. J. Wingham, N. G. Pace, and R. V. Ceen, "An experimental study of the penetration of a water-sediment interface by a parametric beam," J. Acoust. Soc. Am. **79**, 363–374 (1986).
2) T. Kamakura, M. Yoneyama, and K. Ikegaya, "Studies for realization of parametric loudspeaker," J. Acoust. Soc. Jpn. (J) **41**, 378–385 (1985) (in Japanese).
3) G. S. Garrett, J. N. Tjøtta, R. L. Rolleigh, and S. Tjøtta, "Reflection of parametric radiation from a finite plannar target," J. Acoust. Soc. Am. **75**, 1462–1472 (1984).
4) J. Berntsen, J. N. Tjøtta, and S. Tjøtta, "Nearfield of a large acoustic transducer. Part. IV: Second harmonic and sum frequency radiation," J. Acoust. Soc. Am. **75**, 1383–1391 (1984).
5) L. Bjørnø, "Nonlinear acoustics," in *Acoustics and Vibration Progress*, Vol. 2, R. G. B. Stephens and H. G. Leventhall, Eds. (Chapman and Hall, London, 1976), Chap. 4.
6) L. Bjørnø and S. Grinderslev, "Parametric echo scanner for medical diagnosis," J. Phys. Colloq. **C8**, 111–118 (1979).
7) T. Shida, T. Kamakura, and Y. Kumamoto, "Finite amplitude acoustic wave propagation in the medium randomly distributed spherical particles," Meet. Inst. Electron. Inf. Commun. Eng. US87-1 (1987) (in Japanese).